6-17-2004

Selecting Metal Alloy Electric Contact Materials for MEMS Switches

Ronald A. Coutu Jr.
Marquette University, ronald.coutu@marquette.edu

Paul E. Kladitis
Air Force Institute of Technology

Kevin D. Leedy
Air Force Research Laboratory

Robert L. Crane
Air Force Research Laboratory

Accepted version. *Journal of Micromechanics and Microengineering*, Vol. 14, No. 8 (June 17, 2004): 1157. DOI.
Ronald A. Coutu, Jr. was affiliated with the Air Force Institute of Technology, AFIT/ENG, 2950 Hobson Way, Wright Patterson AFB, OH at the time of publication.

Journal of Micromechanics and Microengineering, Vol. 14, No. 8, (June, 2004): 1157-1164. DOI.

Contents

Selecting metal alloy electric contact materials for MEMS switches*

Ronald A. Coutu
Air Force Institute of Technology, Wright Patterson AFB, OH
Paul E. Kladitis
Air Force Institute of Technology, Wright Patterson AFB, OH
Kevin D. Leedy
Air Force Research Laboratory—Sensors Directorate, Wright Patterson AFB, OH
Robert L. Crane
Air Force Research Laboratory—Materials and Manufacturing Directorate, Wright Patterson AFB, OH

Abstract

This paper presents a method for selecting metal alloys as the electric contact materials for microelectromechanical systems (MEMS) metal contact switches. This procedure consists of reviewing macro-switch lessons learned, utilizing equilibrium binary alloy phase diagrams, obtaining thin film material properties and, based on a suitable model, predicting contact resistance performance. After determining a candidate alloy material, MEMS switches were designed, fabricated and tested to validate the alloy selection methodology. Minimum average contact resistance values of 1.17 and 1.87 Ω were measured for micro-switches with gold (Au) and gold–platinum (Au–(6.3%)Pt) alloy electric contacts, respectively. In addition, 'hot-switched' life cycle test results of 1.02×10^8 and 2.70×10^8 cycles were collected for micro-switches with Au and Au–(6.3%)Pt contacts, respectively. These results indicate increased wear with a small increase in contact resistance for MEMS switches with metal alloy electric contacts.

1. Introduction

Radio frequency (RF) microelectromechanical systems (MEMS) switches are paramount in importance for future miniaturizations of RF systems. Space-based radar, phased array radar and phase shifters all depend on being able to easily and reliably switch between different RF loads. Because of their small geometries, exceptional performance and low power consumptions, MEMS metal contact switches are ideally suited for these applications.

Important performance criteria for many MEMS metal contact switch applications are low contact resistance (<1–2 Ω) and high reliability (>10^8 'hot-switched' cycles). The two primary failure mechanisms for metal contact switches are becoming stuck closed (i.e. stiction) or increasing contact resistance with increasing switch cycles. Typically, MEMS metal contact switches use gold-on-gold electric contacts in

order to achieve adequate contact resistance due to gold's low resistivity and resistance to surface oxide and sulfide layers. However, MEMS switches with Au electric contacts are prone to the above failure mechanisms due to gold's relatively low hardness (1–2 GPa). The purpose of this work is to develop a method for selecting metal alloy electric contact materials for micro-switches that are optimized for increased wear, low contact resistance and low susceptibility to oxidation, contaminant gettering and the formation of sulfide layers.

Previous work has concentrated on optimizing mechanical switch designs rather than investigating different electric contact metallurgies.[1] Notable exceptions are Majumder *et al*'s and Duffy *et al*'s utilization of 'platinum group' and platinum electric contact metals, respectively.[2,3] These metals were chosen over gold for their increased hardness and improved wear characteristics. In order to achieve acceptable contact resistance values, Majumder *et al*'s switches required multiple, parallel contacts and were packaged in a novel hermetic environment while Duffy *et al*'s switches required very high actuation voltages (~80 V). Schimkat studied gold–nickel alloy (Au–(5%)Ni) macro-switch contacts in a low-force test configuration but did not fabricate or test actual MEMS devices.[4] Currently, there are no other published works in the open literature describing how to select and incorporate metal alloys as micro-switch electric contact metals. The alloys and compositions presented here were chosen to avoid two-phase alloy regions, intermetallic compounds, the need for high actuation voltages and allow for the testing of unpackaged devices. These considerations help ensure that device fabrication is consistent and repeatable.

The contributions of this work include a procedure for selecting alloy electric contact metallurgies for micro-switches; measured Au–Pd, Au–Pt and Au–Ag thin film material properties; the fabrication of RF MEMS switches with Au–(6.3%)Pt alloy electric contacts, contact resistance measurements and switch life cycle test results.

2. Micro-switch alloy electric contacts

The following section outlines a procedure for choosing alloy electric contact materials suitable for MEMS switches. The general steps of this procedure follow: (1) select candidate alloys by reviewing macro-switch lessons learned, utilizing equilibrium binary alloy phase diagrams and tabulated binary allow bulk material resistivity data, (2) pick an appropriate thin film deposition method and fabricate test specimens, (3) measure important thin film material properties and (4) predict contact resistance performance using a suitable model.

2.1. Select candidate alloys

According to the Metals Handbook, 'no metal has all the desired properties required to accomplish the objectives of different contact applications'.[5] Intuitively, this makes good sense because requirements (i.e. service life, load, etc) change for different applications. Desired electric contact properties include low resistivity, high thermal conductivity, no insulating oxides or sulfides, nominal hardness and elastic modulus, and a high melting point.

Although most metals have been tried, silver and its alloys are the most widely used macro-switch electric contact materials because of their superior electrical, mechanical and thermodynamic properties. One drawback to using silver is that it tarnishes in the presence of sulfur and forms mechanically robust surface sulfide layers. Although, not a big problem for macro-switches, where many

Newtons of contact force are available to penetrate nonconductive surface layers, in micro-switches pure silver or alloys with high percentages of silver are not suitable electric contact materials.

Gold contacts, on the other hand, are widely used in micro-switches due to its low resistivity, high oxidation resistance and easy integration with available device fabrication processes. Gold, however, is a very soft metal, has a low melting point and adsorbs carbonaceous layers. These properties make gold electric contacts prone to erosion and wear.[5] Although gold is a soft metal, it can be hardened using alloying elements or solutes such as nickel (Ni), palladium (Pd), silver (Ag) or platinum (Pt) to help minimize contact wear and erosion.[5] The resulting alloys are best suited for low current applications because of their relatively low melting points.[5]

These macro-switch lessons learned form the basis for investigating gold alloy contact metals for MEMS switches. Phase diagrams and bulk resistivity values were used to further investigate binary alloys and determine specific gold alloy compositions.

A wealth of knowledge, pertinent for designing MEMS switches, is gained by using binary alloy phase diagrams.[6] Important considerations, specific for micro-switches, will be discussed. Using the phase diagrams, single-phase alloys and miscibility regions are located. Single-phase alloys are desired because metal alloy crystal structures in these areas do not physically change with elevated temperature. Miscibility gaps or two-phase regions should be avoided to (1) ensure that contact alloys are reliably deposited during device fabrication and (2) to avoid brittle, highly resistive, intermetallic compounds that may inadvertently be formed. Miscible gold alloys made from low concentrations of alloying elements are desirable to avoid depositing intermetallic compounds during device fabrication.

Most binary metal alloys obey Matthiessen's rule where the relationship between resistivity and alloy composition is parabolic and a trade-off situation often exists between bulk resistivity and other material properties such as hardness or elastic modulus.[5,7]

Schimkat tested gold–nickel alloy (Au–(5%)Ni) macro-switch electric contacts under low contact force (100–600 µN) conditions.[4] He theorized that Au–Ni alloys were useful micro-relay contact materials. In figure 1, however, the Au–Ni phase diagram shows two stable alloy phases across the entire composition range below 810.3 °C.

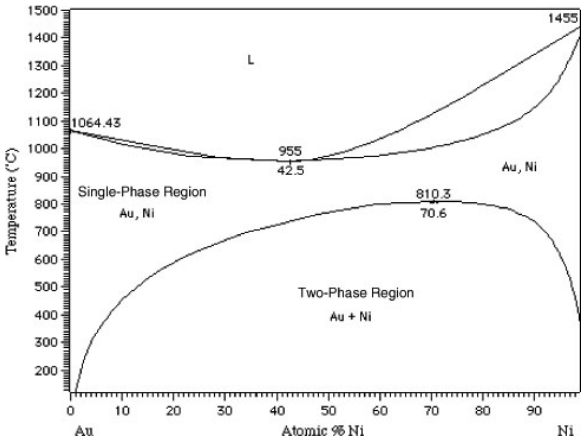

Figure 1. Equilibrium binary alloy phase diagram for gold–nickel alloys.[6]

The miscibility gap or two-phase region, shown in figure 1, indicates that Au–Ni alloys are not necessarily the best choice for micro-switch electric contacts because intermetallics and unpredicted material second phases will almost certainly be present. This hypothesis is supported by erratic bulk resistance ratios, found in the CRC Handbook, that do not follow Matthiessen's rule.[7] The alloy composition that Schimkat tested was a stable, two-phase material. Due to variations in the metal alloy deposition process (i.e. temperature, pressure, etc), however, this precise Au–Ni composition is extremely difficult to reliably duplicate and incorporate into micro-switch fabrication processes.

Figures 2–4 are the phase diagrams for Au–Pd, Au–Ag and Au–Pt alloys, respectively. The Au–Pd phase diagram shows one stable alloy phase below 1064.43 °C and three known regions where intermetallic compounds form. Single-phase Au–Pd alloys normally result when using Pd concentrations of less than ~10%.

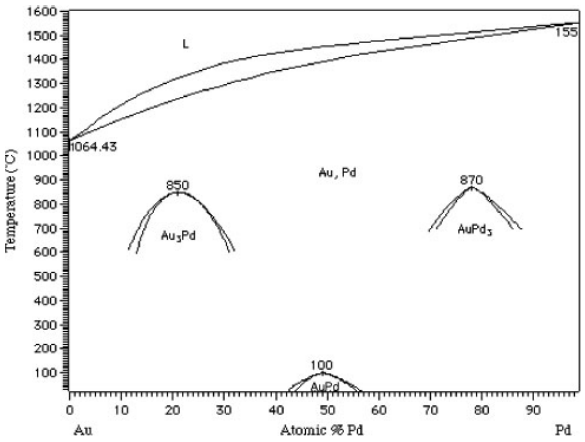

Figure 2. Equilibrium binary alloy phase diagram for gold–palladium alloys.[6]

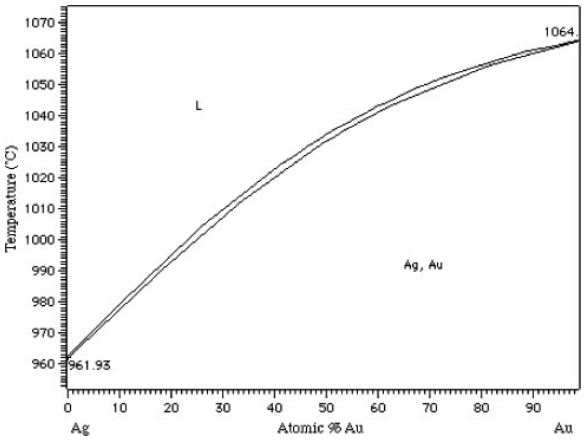

Figure 3. Equilibrium binary alloy phase diagram for gold–silver alloys.[6]

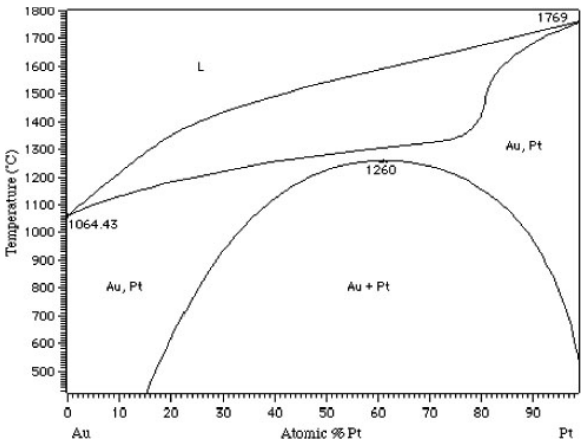

Figure 4. Equilibrium binary alloy phase diagram for gold–platinum alloys.[6]

The Au–Ag phase diagram shows one stable material phase for all alloy compositions. The melting temperature for Au–Ag alloys increases from 961.93 to 1064.00 °C as the Au concentration increases from 0 to 100%. Miscible Au–Ag alloys with Ag concentrations less than ~30% are less likely to tarnish in the presence of sulfur.[5] In this study, Au–Ag alloys with less than ~15% silver content were considered.

The Au–Pt phase diagram shows two stable phases below 1260 °C but only with platinum (Pt) concentrations greater than ~15%. Single-phase Au–Pt alloys result for Pt concentrations of less than ~15%.

The information from the phase diagrams (figures 2–4), along with low bulk material resistivity values, found in the CRC Handbook of Electrical Resistivities of Binary Metallic Alloys, indicates that Au–Pd, Au–Ag and Au–Pt alloys are viable candidates for micro-switch electric contacts.[7]

There were several other possible metals that could potentially be alloyed with either gold, platinum or palladium to form micro-switch electric contacts. The most notable are rhenium (Re), ruthenium (Ru), rhodium (Rh), iridium (Ir), copper (Cu) and cobalt (Co).[8] Gold–rhenium (Au–Re) and gold–iridium (Au–Ir) alloys were not considered because alloy phase diagrams were not available for these material combinations.[6] Phase diagrams for gold–rhodium (Au–Rh), platinum–rhodium (Pt–Rh), platinum–iridium (Pt–Ir), palladium–ruthenium (Pd–Ru) and platinum–palladium (Pt–Pd) alloys were available; however, the bulk material resistivities, found in the CRC Handbook, were much greater than those for the Au–Pd, Au–Ag and Au–Pt alloys.[7] Phase diagrams were also available for gold–ruthenium (Au–Ru), platinum–rhenium (Pt–Re), platinum–ruthenium (Pt–Ru), palladium–rhenium (Pd–Re), palladium–rhodium (Pd–Rh), palladium–iridium (Pd–Ir), rhenium–ruthenium (Re–Ru), ruthenium–iridium (Ru–Ir) and rhodium–iridium (Rh–Ir) alloys; however, bulk material resistivities were not available for these alloys.[7] Gold–copper (Au–Cu) alloys were not considered because alloys with high concentrations of Cu have a tendency to form robust surface films while alloys with low concentrations of Cu are known to form intermetallic compounds.[6] Gold–cobalt (Au–Co) alloys were also not considered because, like Au–Ni alloys, the two-phase region extends across the entire alloy composition spectrum making reliable, repeatable thin-film deposition difficult.[6]

Additionally, gold–titanium (Au–Ti) alloys were not used in this study. Although titanium (Ti) is a popular adhesion metal for gold, particularly for lower switch contacts, it is not a suitable micro-switch electric

contact metal. This is due to the numerous miscibility gaps and intermetallic compounds, shown in figure 5, that are present whenever Au is deposited directly onto Ti.

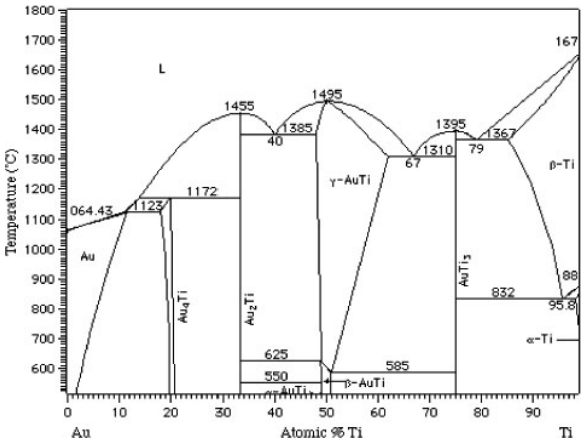

Figure 5. Equilibrium binary alloy phase diagram for gold–titanium alloys.[6]

For example, with a composition of 49% Au and 51% Ti, the material physically changes from the β-Au–Ti alloy to the γ-Au–Ti alloy when the temperature increases above ~590 °C. Similar metallurgical changes occur when a gold top layer is mechanically worn away from a switch's lower electric contact with high numbers of switch cycles.

Macro-switch lessons learned, equilibrium binary alloy phase diagrams and bulk material resistivity values are important tools for evaluating potential material combinations for MEMS switch electric contacts. In addition to using single-phase binary alloys, avoiding intermetallic compounds and materials combinations that tarnish, oxidize or form robust surface films, alloy deposition techniques must be compatible and easily integrated with available micro-switch fabrication processes.

2.2. Thin film deposition

Thin metal films are routinely deposited using either physical vapor deposition (PVD) or chemical vapor deposition (CVD) methods.[9,10] The PVD techniques of sputtering and evaporation, accomplished under vacuum, can be used for depositing metal alloy thin films. Alloy deposition using CVD is more difficult because of its precise stoichiometric dependence.

In general, evaporative metal deposition involves heating a material to its melting point and allowing the vaporized atoms, traveling in straight lines, to impinge and condense on a target substrate. Alloys are deposited by using either a single-alloyed material container or by using co-evaporation where two different materials are heated simultaneously. Precise composition control is difficult when evaporating a single container alloy because different metals have different vapor pressures and therefore different evaporation rates. When using co-evaporation obtaining uniform alloy composition, across the target substrate, is difficult because of straight line evaporation patterns and vapor phase material scattering.[10]

Sputtering is a process where inert gas ions (i.e. argon (Ar)) are used to bombard a material target in the presence of an electric field. Once the ions hit the target with sufficient energy, material is dislodged due to an exchange of momentum. The dislodged material is then transported to the substrate ballistically.[9] Like evaporation, alloys can be sputter deposited using either alloyed material targets or by

co-sputtering individual materials. Unlike evaporation, however, alloy compositions are better controlled when sputtered because transition to vapor phase is not required.

In this work, a Denton Discovery-18 sputtering system was used to co-sputter the thin metal alloy films. The procedure for co-sputtering the alloy films was to first characterize the deposition rates for the individual alloy components and then co-sputter at appropriate power levels. Deposition rates were determined through an iterative process of choosing a chamber pressure, setting the cathode power for an estimated film thickness, verifying film thickness using a Tencor P-10 Surface Profiler and finally adjusting the cathode power level. With these data, deposition rate versus cathode power was plotted and curve fitted. The curve fit equations were then used to estimate cathode power level settings needed to deposit the alloy films. Three different Au–Pd, Au–Ag and Au–Pt test specimens (~500 Å thick) were co-sputtered onto 3 inch silicon (100) test wafers using this procedure. Material property testing was accomplished to verify that single-phase alloys were deposited and two-phase regions and intermetallic compounds were avoided. Thin film material properties, not available in the open literature, were measured directly to ascertain important electrical and mechanical properties.

2.3. Material property testing

A premise of this study is that suitable MEMS switch electric contacts are realizable when using miscible (i.e. alloy elements are completely soluble in each other), single-phase alloys and avoiding two-phase regions and intermetallic compounds. X-ray photoelectron spectroscopy (XPS) and x-ray diffraction (XRD) were used to evaluate miscibility and composition of the co-sputtered metal alloy films. A detailed crystallography study and compositional analysis were not performed. XPS was used to compare actual atomic composition percentages to those predicted prior to deposition and XRD was used to identify material 2θ lines. Nanoindenting and four-point probe resistance measurements were used to assess thin film hardness and resistivity, respectively, and a surface profiler was used to evaluate surface roughness.

XPS was used to verify the alloy composition of each test specimen and investigate the contaminant layers. For example, the composition of the Au–(1%)Pt alloy film was approximately 97.8% Au and 2.2% Pt. The alloy composition measurements for the remaining candidate alloys are presented in table 1.

Table 1. XPS composition measurements for the Au–Pt, Au–Pd and Au–Ag test specimens.

Predicted	XPS measured
Au–(1%)Pt	Au(97.8%)–(2.2%)Pt
Au–(2%)Pt	Au(93.7%)–(6.3%)Pt
Au–(5%)Pt	Au(89.9%)–(10.1%)Pt
Au–(1%)Pd	Au(99.3%)–(0.7%)Pd
Au–(3%)Pd	Au(98.5%)–(1.5%)Pd

Au–(5%)Pd	Au(96.3%)–(3.7%)Pd
Au–(5%)Ag	Au(97.9%)–(2.1%)Ag
Au–(7%)Ag	Au(94.8%)–(5.2%)Ag
Au–(10%)Ag	Au(93.6%)–(6.4%)Ag

All the candidate alloy test specimens were within the single-phase ranges shown in the phase diagrams (figures 2–4).

A contaminant layer approximately 20–40 Å thick, consisting of carbon (C) and oxygen (O), was present on each of the test specimens. XPS depth profiling (i.e. calibrated sputter cleaning) was used to determine the thickness and composition of the contaminant layer. Sulfur (S) was not present on any of the samples.

XRD was accomplished on all test specimens to evaluate whether single-phase alloys or intermetallic compounds were deposited. For example, measured (111) crystal orientation 2θ lines, for sputtered Au, Pt and Au–(2.2%)Pt films, were approximately 38.30°, 39.92° and 38.40°, respectively. Since the alloy film had only a single 2θ line, shifted slightly towards the Pt line, intermetallic compounds were not present. All the alloy thin film specimens were tested using XRD and no intermetallic compounds were observed.

In this study, material hardness was measured using traditional nanoindenting techniques with a MTS Nanoindentor IIs. Ten indents were measured on each of the test specimens. Substrate effects were minimized by limiting the indent depth to approximately 10–15% of film's overall thickness. Table 2 presents the hardness data for the sputtered Au–Pt, Au–Pd and Au–Ag test specimens. Au, Pt, Pd and Ag measurements are provided for comparison.

Table 2. Nanoindentor IIs hardness (*H*) measurements for Au, Pt, Pd, Ag, Au–Pt, Au–Pd and Au–Ag test specimens.

Material	*H* (GPa)	Standard deviation (GPa)
Au	1.77	0.18
Pt	3.55	0.25
Pd	2.87	0.22
Ag	1.31	0.09
Au–(2.2%)Pt	1.69	0.11

Au–(6.3%)Pt	2.19	0.26
Au–(10.1%)Pt	1.98	0.10
Au–(0.7%)Pd	1.64	0.07
Au–(1.5%)Pd	1.87	0.21
Au–(3.7%)Pd	1.96	0.13
Au–(2.1%)Ag	1.82	0.10
Au–(5.2%)Ag	1.68	0.14
Au–(6.4%)Ag	1.73	0.16

A standard four-point probe system was used to collect thin film resistivity measurements. Ten resistivity measurements were collected across each of the alloy test wafers to ensure uniform material deposition. Tables 3 presents the resistivity data collected for the Au–Pt, Au–Pd and Au–Ag films. Au, Pt, Pd and Ag measurements are provided for comparison.

Table 3. Resistivity measured using the four-point probe method for the Au, Pt, Pd, Ag, Au–Pt, Au–Pd and Au–Ag test specimens.

Material	Resistivity (μΩ cm)	Standard deviation (μΩ cm)
Au	3.93	0.0004
Pt	13.88	0.0015
Pd	13.75	0.0006
Ag	1.78	0.0001
Au–(2.2%)Pt	5.83	0.0006
Au–(6.3%)Pt	7.17	0.0001

Au–(10.1%)Pt	10.60	0.0015
Au–(0.7%)Pd	5.14	0.0005
Au–(1.5%)Pd	5.70	0.0003
Au–(3.7%)Pd	6.37	0.0002
Au–(2.1%)Ag	5.28	0.0006
Au–(5.2%)Ag	5.69	0.0015
Au–(6.4%)Ag	6.20	0.0004

Surface roughness root mean square (RMS) values between 30 and 50 Å, typical of sputtered metal films, were measured for each of the test specimens using a Tencor P-10 surface profiler.

Once miscible alloy deposition was verified and the hardness and resisivity measurements accomplished, a contact resistance metric was used to determine which alloy was best suited for incorporation into the micro-switch fabrication process.

2.4. Contact resistance performance prediction

The contact resistance that results from making an electrical connection is defined by equation (1) which considers the effects of constriction (R_c) and contaminant film (R_{cf}) resistances:[11]

$$R_C = R_c + R_{cf}. \qquad (1)$$

Constriction resistance, due to contact surface topography or roughness, is modeled analytically using the Maxwellian spreading resistance theory:[11]

$$R_c = \frac{\rho}{2r_{eff}} \qquad (2)$$

where R_c is the constriction resistance, ρ is the resistivity and r_{eff} is the effective radius of a circular contact area. Equation (2) assumes that current flow is completely attributed to diffusive electron transport.[11] When contact material deformation is assumed to be plastic, equation (2) is revised, using Abbott and Firestone's material deformation model,[12] resulting in the well-known Holm's contact resistance equation:

$$R_c = \frac{\rho}{2}\sqrt{\frac{H\pi}{F_c}} \qquad (3)$$

where F_c is the contact force.[11] Table 4 is a summary of predicted contact resistance, calculated using equation (3), measured hardness (table 2) and measured resistivity (table 3) values, for the candidate alloy electric contact materials. A contact resistance prediction for sputtered gold electric contacts is also provided for comparison. The contact surfaces were assumed to be 'clean' (i.e. free of contaminate film layers) with a normally applied contact force of 50 µN.

Table 4. Minimum contact resistance (R_c) predictions for candidate electric contact materials.

Metal/alloy	Predicted minimum, R_c (Ω)
Au	0.21
Au–(2.2%)Pt	0.30
Au–(6.3%)Pt	0.42
Au–(10.1%)Pt	0.59
Au–(0.7%)Pd	0.26
Au–(1.5%)Pd	0.31
Au–(3.7%)Pd	0.35
Au–(2.1%)Ag	0.28
Au–(5.2%)Ag	0.29
Au–(6.4%)Ag	0.32

Observe from tables 2 and 4 that Au–(6.3%)Pt alloy has a predicted contact resistance that is comparable to Au and it also has the highest measured hardness value. Based on this, MEMS test structures (i.e. micro-switches) with Au–(6.3%)Pt electric contacts were designed, fabricated and tested to investigate the feasibility of using alloy electric contacts and validate the procedure for selecting alloy contact metals.

3. MEMS switches

The design, fabrication and test results of cantilever-style MEMS switches with Au–(6.3%)Pt electric contacts are discussed next.

3.1. Design

In metal contact micro-switches, initial switch closure is defined by the pull-in voltage. At pull-in, physical contact between the switch's upper (i.e. dimples) and lower electric contacts is first established with minimal contact force. As the micro-switch's actuation voltage is increased, the cantilever beam bends, contact force increases and material deformation causes the contact area to increase. Contact area friction, due to cantilever beam bending, tends to mechanically clean (i.e. 'wiping') contaminant films from the electric contact's surface.

Previous work by this author showed that the contact force bounded by pull-in and collapse voltages could be analytically modeled using the beam illustrated in figure 6.[13]

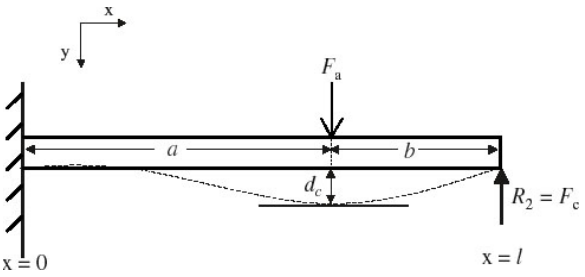

Figure 6. Cantilever beam model with a fixed end at $x = 0$, a simply supported end at $x = l$ and an intermediately placed external load (F_a) at $x = a$.

The applied load is modeled as an electrostatic force:

$$F_e = \frac{\epsilon_o A_{sa} V^2}{2g^2} \qquad (4)$$

where F_e is the electrostatic force, ϵ_o is the permittivity of free space, A_{sa} is the surface area of one parallel plate, V is the actuation voltage and g is the gap between the parallel plates.[14] F_e is represented by F_a in figure 6.

Equation (5) is the resulting contact force equation:

$$F_c = \frac{F_a}{2l^3} a^2 (3l - a) \qquad (5)$$

where F_c is the contact force, F_a is the applied electrostatic force, a is the location of the applied electrostatic force and l is the beam length.[15] This simple model does not consider either beam tip deflection or contact material deformation after switch closure or pull-in. A more detailed contact force model results when electric contact material deformation, assumed to be elastic, plastic or elastic–plastic [16], and beam tip deflection are considered.[17]

After selecting a candidate alloy (Au–(6.3%)Pt) and a compatible deposition process (i.e. co-sputtering), micro-switches were designed, using equations (4) and (5) and fabricated using a custom process.

3.2. Fabrication

Cantilever-style micro-switches, shown in figure 7, with Au–(6.3%)Pt electric contacts were fabricated on highly resistive sapphire substrates using a custom fabrication process. For comparison, micro-switches with sputtered Au electric contacts were also fabricated.

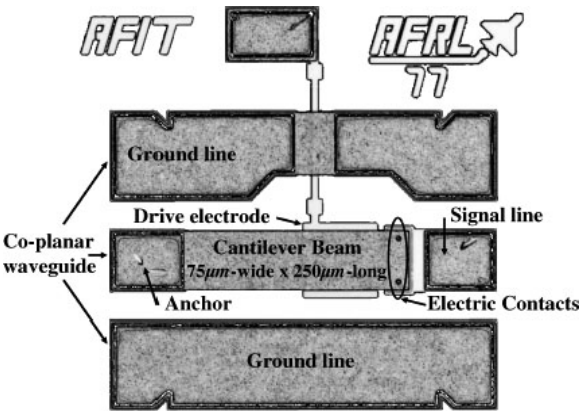

Figure 7. A captured video image of a 75 µm wide by 250 µm long RF MEMS metal contact switch with Au–(6.3%)Pt electric contacts.

Table 5 summarizes the fabrication process and the typical layer thicknesses.

Layer	Material	Thickness (µm)
Electrode	Evaporated gold	0.3
Lower contact	Evaporated gold/sputtered metal alloy	0.3
Beam gap	Created from sacrificial photoresist	3.0
Contact gap	Created from sacrificial photoresist	2.0
Upper contact (i.e. dimple)	Sputtered metal alloy	0.05
Beam	Electroplated gold	5.0
Co-planar waveguide	Evaporated gold/electroplated gold	5.3

The drive or actuation electrode and the lower electric contact is planar while the upper contact bump or dimple is hemispherical. The electrode and lower contact layer was evaporated, patterned using photolithography and then excess material was removed using a standard lift-off technique.[9] A thin chromium (Cr) adhesion layer was used under the evaporated Au layer. The lower contact metal, sputter deposited on top of the evaporated layer, was patterned using photolithography and then excess

material was removed using a lift-off technique. The beam gap was created from a sacrificial photoresist layer. The beam's hinge geometry and upper contact dimples were defined in the sacrificial photoresist using standard photolithography. A timed re-flow in an oven was used to reform, by surface tension, the usual 'plug-shaped' dimple into a hemisphere-shaped contact bump like those shown in figure 8.

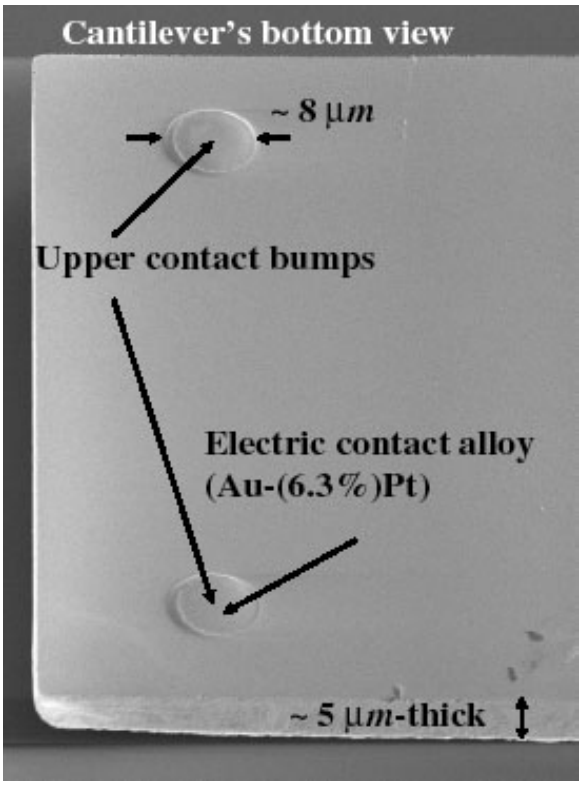

Figure 8. Scanning electron micrograph (SEM) image of a 'flipped' over cantilever showing the alloy contact material on the hemispherical-shaped upper contact bumps located underneath the beam.

The upper contact metals were sputter deposited and patterned using photolithography. The excess metal, however, was removed using an etch back technique, instead of lift-off, to avoid damaging the sacrificial photoresist layer. After electroplating the cantilever's gold structural layer, the devices were released using a CO_2 critical point dryer and tested to ensure proper device operation and performance.

3.3. Testing

A series of micro-switches, like that shown in figure 7, were tested to experimentally characterize the contact resistance and lifetime for micro-switches with Au and Au–(6.3%)Pt electric contacts. The micro-switches were tested by wafer probing using a Alessi Rel-4100A Microprobe Station with standard microprobes. The actuation voltage, applied using an HP 3245A universal source and a Krohn–Hite wideband amplifier, was swept from 0 to 110 V in 0.5 V increments. Closed switch resistance was measured using an HP 3458A multimeter in a four-point probe configuration. Contact resistance was determined by subtracting the measured resistance of the cantilever beam from the measured closed switch resistance values. Figure 9 is a schematic illustration of the experimental setup.

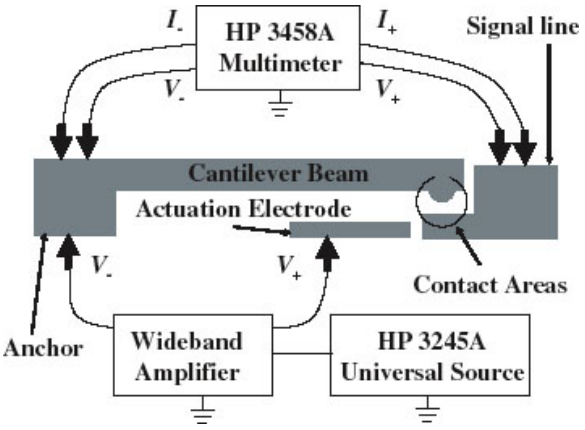

Figure 9. Experimental test setup used to measure the contact resistance (R_c) and collect micro-switch life cycle data.

During contact resistance testing, ten individual micro-switches were tested by applying a bias or actuation voltage between the cantilever beam and the drive electrode. The micro-switch closed when the magnitude of the bias voltage exceeded the pull-in voltage. As the applied bias was increased beyond the pull-in voltage, the contact force increased until the beam collapsed onto the drive electrode at the collapse voltage. The maximum contact force and minimum contact resistance occurred just prior to reaching the beam collapse voltage. Once collapse was reached, the switch shorted out and was no longer operable. Table 6 summarizes the minimum average contact resistance (R_c) for MEMS switches with sputtered Au and Au–(6.3%)Pt electric contacts.

Table 6. Average minimum contact resistance measurements for MEMS switches with Au and Au–(6.3%)Pt electric contacts.

Metal/alloy	Minimum average R_c (Ω)	Standard deviation (Ω)
	1.17	0.14
Au–(6.3%)Pt	1.87	0.37

During life cycle testing, selected micro-switches were operated continuously just below the resonant frequency (50 kHz) with an actuation voltage set to the pull-in voltage plus ~1–3 V for increased contact force. The devices were cycled until they either failed open (i.e. infinite resistance) or closed (i.e. stuck down). During each switch actuation, the devices were 'hot switched' with the multimeter's open circuit voltage (~8.2 V). The success criteria were contact resistance values less than approximately 3 Ω. Contact resistance versus switch cycle raw data, for selected micro-switches, was curve fitted and the resulting trendlines were plotted in figure 10.

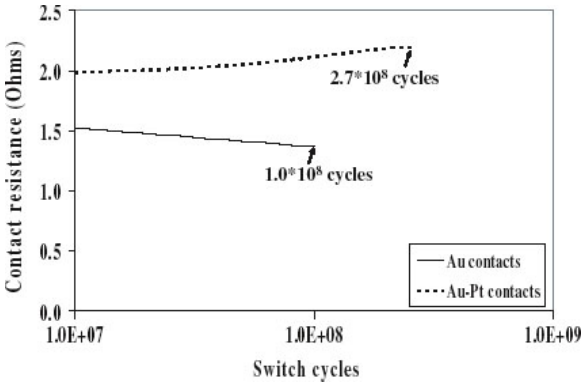

Figure 10. Contact resistance versus switch cycles data plot.

Generally, micro-switches with Au electric contacts are limited to approximately 10^6 'hot-switched' cycles because evaporated Au is a soft metal and prone to wear.[2] Majumder *et al* report greater than 10^7 'hot-switched' cycles and approximately 10^{11} 'cold-switched' cycles for devices with a 'platinum group' electric contact metal.[2] The micro-switches with Au–(6.3%)Pt contacts were 'hot-switched' and resulted in contact resistance between 1.5 and 2.2 Ω and, when compared to micro-switches with sputtered Au electric contacts, exhibited approximately a 2.7 times increase in switching lifetime. This was most likely due to the increased material hardness of the sputtered alloy contact films. Also, the micro-switches with sputtered Au contacts, in this work, outperformed other micro-switches with evaporated Au contacts.[2] Once again, this was most likely due to the increased material hardness of the sputtered Au contact metals. The measured Meyer hardness of evaporated Au, sputtered Au and co-sputtered Au–(6.3%)Pt thin films (500 Å thick) were approximately 1, 2 and 2.2 GPa, respectively.

The micro-switches with Au–(6.3%)Pt contacts exhibited an increase in contact resistance with increased numbers of switch cycles. Figure 10 shows a rise in contact resistance between approximately 3×10^7 and 2.7×10^8 switch cycles. This may indicate that a contaminant film layer, induced by contact wear, was developing.

4. Conclusions

This paper presents a method for selecting metal alloys as the electric contact materials for MEMS contact switches. This procedure consists of reviewing macro-switch lessons learned, utilizing equilibrium binary alloy phase diagrams, obtaining thin film material properties and, based on a suitable model, predicting contact resistance performance.

MEMS switches with Au–(6.3%)Pt electric contacts were designed, fabricated and tested to validate the metal alloy selection methodology. Minimum average contact resistance values of 1.17 and 1.87 Ω were measured from micro-switches with Au and Au–(6.3%)Pt alloy electric contacts, respectively. 'Hot-switched' life cycle tests, for selected devices, resulted in 1.02×10^8 and 2.70×10^8 cycles for micro-switches with Au and Au–(6.3%)Pt alloy electric contacts, respectively. MEMS switches with alloy electric contacts, when compared to micro-switches with Au contacts, have similar contact resistance and increased life cycle performance. This indicates that the selection methodology for metal alloy electric contacts is suitable for MEMS switches.

Acknowledgments

This work was sponsored by the Materials and Manufacturing Directorate, Air Force Research Laboratory, USAF, under project order number QGWSML02722002, POC: Dr Robert L Crane. The authors would also like to acknowledge the Sensors Directorate, Air Force Research Laboratory, in particular, Dr Jack Ebel, Dr Rick Strawser and Dr Becky Cortez for their encouragement and suggestions.

Footnotes

*The views expressed in this paper are those of the authors and do not reflect the official policy or position of the United States Air Force, Department of Defense, or the US Government.

References

1. Peroulis D et al 2003 *IEEE Trans. Microw. Theory Tech.* **51** 259-70
2. Majumder S et al 2003 *IEEE Instrum. Meas. Mag.* March 12-15
3. Duffy S et al 2001 *IEEE Microw. Wirel. Compon. Lett.* **11** 106-8
4. Schimkat J 1999 *Sensors Actuators* A **73** 138-43
5. Committee Handbook 1990 *Metals Handbook* vol 2 10th edn (USA: ASM International)
6. Okamato H et al 1992 *Binary Alloy Phase Diagrams* 2nd edn (OH: ASM International)
7. Schroder K 1983 CRC *Handbook of Electrical Resistivities of Binary Metallic Alloys* (Boca Raton, FL: CRC Press)
8. Rebeiz G 2003 RF *MEMS Theory, Design, and Technology* (NJ: Wiley)
9. Madou M 2002 *Fundamentals of Microfabrication* 2nd edn (Boca Raton, FL: CRC Press)
10. Bunshah R 1982 *Deposition Technologies for Films and Coatings: Developments and Applications* (NJ: Noyes Publications)
11. Holm R 1969 *Electric Contacts: Theory and Applications* (Berlin: Springer)
12. Abbot E and Firestone F 1933 *ASME Mech. Eng.* **55** 569
13. Coutu R Jr et al 2003 *Proc. Eurosensors XVII (Guimarães, Portugal)* pp 64-7
14. Kovacs G 1998 *Micromachined Transducers Sourcebook* (New York: McGraw-Hill)
15. Shigley J and Mischke C 1990 *Mechanical Engineering Design* 5th edn (New York: McGraw-Hill)
16. Chang W 1997 *J. Wear* **212** 229-7
17. Coutu R Jr and Kladitis P 2003 Proc. *NSTI Nanotech 2004* (Boston, MA) vol 2 pp 219-23